Engineering Fracture Mechanics 96 (2012) 588–605

Contents lists available at SciVerse ScienceDirect

Engineering Fracture Mechanics

journal homepage: www.elsevier.com/locate/engfracmech

Prediction of remaining useful life for fatigue-damaged structures using Bayesian inference

Jaydeep M. Karandikar [a], Nam Ho Kim [b], Tony L. Schmitz [a,*]

[a] Department of Mechanical Engineering and Engineering Science, University of North Carolina at Charlotte, Charlotte, NC, USA
[b] Department of Mechanical and Aerospace Engineering, University of Florida, Gainesville, FL, USA

ARTICLE INFO

Article history:
Received 7 May 2012
Received in revised form 30 August 2012
Accepted 15 September 2012

Keywords:
Crack growth
Fatigue loading
Bayesian inference
Uncertainty
Remaining useful life

ABSTRACT

Structural health monitoring enables fatigue damage for in-service structures to be evaluated and the remaining useful life to predicted. In this paper, Bayesian inference using a random walk method was implemented to predict the remaining useful life of an aircraft fuselage panel subjected to repeated pressurization cycles. The Paris' law parameters, m and C, were treated as uncertain along with the initial crack size, a_0. Random samples from the joint distribution of m, C, and a_0 were used to generate the fatigue crack growth curve using Paris' law. Using simulated crack size data, the probability that a selected fatigue crack growth curve represented the true fatigue crack growth curve was updated. Crack sizes were calculated using Paris' law with uncertain parameters and random noise and bias were added to the simulated crack sizes. With this approach, fatigue crack size was characterized by a probability distribution at each loading cycle. A detailed explanation of Bayesian updating using the random walk method is provided. crack size. The effect of the likelihood on the remaining useful life predictions was also evaluated. The proposed method takes into account model uncertainties as well as the presence of noise and bias in the measurement data.

1. Introduction

Structural health monitoring (SHM) is the process of identifying damage in civil, aerospace, and mechanical engineering structures [1,2]. SHM provides automated damage diagnosis by combining damage detection algorithms with structural monitoring systems [3]. In aerospace structures, such as a fuselage panel in an aircraft, SHM enables in-service fatigue damage to be monitored and diagnosed. In this case, the aircraft fuselage is subjected to fatigue loading due to pressurization cycles during each flight. In general, fatigue damage refers to the nucleation and growth of microstructure cracks, such as dislocations, to detectable macrostructure cracks. For aircraft structures, the crack size information provided by the SHM sensor can be used to predict the remaining useful life (RUL), or the number of cycles until a crack reaches the critical value. Accurate RUL estimation is useful for scheduling maintenance and visual inspections. However, uncertainty always exists in the RUL estimates due to uncertainty in the crack growth model, material and geometric properties, initial crack size, measured crack size (due to uncertainty in the SHM sensor measurements), and fatigue load values. The accuracy of the SHM data is relatively low compared to non-destructive inspection/evaluation (NDI/E) techniques because the SHM sensor data may have a bias and/or noise; the former is due to calibration error, sensor location, or device error, while the latter is due to the measurement environment and sensor limitations [4]. Due to the inherent uncertainty in RUL, it should be reported together with the associated uncertainty [5]. An important consideration in SHM-based prognosis is therefore to accurately

* Corresponding author.
E-mail address: tony.schmitz@uncc.edu (T.L. Schmitz).

0013-7944/$ - see front matter © 2012 Elsevier Ltd. All rights reserved.
http://dx.doi.org/10.1016/j.engfracmech.2012.09.013

Nomenclature

a	half crack size
B	true bias in the in the half-crack size measurements
C	Paris' law parameter
k	parameter in the likelihood function
l	likelihood function
m	Paris' law parameter
M	true mean of the noise in the half-crack size measurements
n	number of sample fatigue curves
N	number of cycles
S	true standard deviation of the noise in the half-crack size measurements
U	uniform distribution
r	fuselage radius
t	panel thickness
σ	user estimated standard deviation in the half-crack size measurements
da/dN	crack growth rate
a_0	initial half crack size
a_c	critical half-crack size
a_{meas}	measured half-crack size
a_N	half crack size after N cycles
b_1	user estimated bias in the half-crack size measurements
b_2	user estimated bias in the half-crack size measurements
K_{IC}	plane strain fracture toughness
N_f	the number of cycles when the crack size reaches the critical crack size or the number of cycles to failure
$\hat{N}$	normal distribution
$p(a)$	probability of the half-crack size being less than the selected half-crack size value
$p(a < a_c)$	probability of the half-crack size being less than the critical half-crack size value
$P(A\|\&)$	prior distribution about an uncertain event, A, at a state of information, &
$P(B\|A, \&)$	likelihood of obtaining an experimental result B given that event A occurred
$P(B\|\&)$	probability of receiving experimental result B (without knowing A has occurred)
$P(A\|B, \&)$	posterior belief about event A after observing the experiment results, B
$P(m)$	posterior probabilities for m
$P(C)$	posterior probabilities for C
$P(m, C)$	posterior probabilities for $\{m, C\}$ pairs
RUL	remaining useful life
ΔK	range of stress intensity factor
Δp	pressure differential
$\Delta\sigma_h$	range of hoop stress
μ_m	mean values of m
μ_C	mean value of C
$\rho_{m,C}$	correlation coefficient between m and C
σ_h	hoop stress
σ_m	standard deviations of m
σ_C	standard deviation of C

predict remaining life in the presence of uncertainty. Physics-based models capture the dynamics of fatigue crack growth. However, they are deterministic and do not generally incorporate uncertainty [6–9]. To address this issue, various methods to address uncertainty in fatigue have been proposed, such as stochastic modeling [10–15], particle filters [16–18], and Bayesian inference [4,19–21]. In particular, Coppe et al. used Bayesian inference to progressively reduce the uncertainty of the Paris' law parameters using sensor measurement with noise and bias. The posterior probability distributions were used to predict RUL [4]. Perrin et al. applied Markov Chain Monte Carlo simulation using the Metropolis algorithm to perform Bayesian updating of the Paris' law parameters [19]. Mohanti et al. used a multivariate Gaussian process, which is a Bayesian statistic stochastic model [20]. Zhang and Mahadevan used a Bayesian procedure to quantify uncertainty in: mechanical and statistical model selection; and the distribution parameters to predict the fatigue reliability [21].

Bayesian methods have increased in popularity in recent years. Bayesian inference provides a normative and formal method of belief updating when new information, in the form of experimental results for example, becomes available. The objective of this paper is to demonstrate and validate the random walk Bayesian inference technique for predicting RUL of an aircraft fuselage panel subjected to repeated pressurization cycles. Paris' law for crack growth with two parameters, an exponent, m, and a y-intercept, C, was used in this study [22,23] to demonstrate the method; the method can also be

applied to more advanced models with additional parameters. Simulated crack size data was used to update the probability crack size distributions and the uncertain crack growth model parameters using Bayes' rule. The proposed method takes into account uncertainties in the sensor measurement, crack growth model parameters, m and C, and the initial half-crack size. Section 2 briefly summarizes Paris' damage growth model for completeness. Bayes' rule is described in Section 3. The Bayesian inference method using random walks is described in Section 4. Section 5 shows the RUL predictions. Advantages are discussed in Section 6 and conclusions are provided in Section 7.

2. Damage growth model

Microstructure cracks, such as dislocations, always exist in a structure. Fatigue loading can cause these microstructure-level cracks to grow into macrostructure-level cracks. In this study, Paris' law was used to model crack growth in a fuselage panel subjected to constant amplitude fatigue loading from repeated pressurization cycles. Paris' law was selected because it is commonly used for fatigue analysis due to its simplicity [4,21,24–26]. Paris' law is given by [22]:

$$\frac{da}{dN} = C(\Delta K)^m \tag{1}$$

where a is the half-crack size in m, N is the number of cycles, $\frac{da}{dN}$ is the crack growth rate in meters/cycle, ΔK is the stress intensity factor range in MPa $\sqrt{m}$, and m and C are the damage growth parameters. The stress intensity factor range for a center-cracked panel is calculated using Eq. (2). Note that Eq. (2) does not include any correction factor due to the assumed finite size of the fuselage panel. The range of hoop stress, $\Delta\sigma_h$, due to the pressure differential, Δp, is given by Eq. (3), where r is the fuselage radius and t is the panel thickness.

$$\Delta K = \Delta\sigma_h\sqrt{\pi a} \tag{2}$$

$$\Delta\sigma_h = \frac{(\Delta p)r}{t} \tag{3}$$

The number of fatigue loading cycles required to grow a crack from the initial half-crack size, a_0, to the final half-crack size, a_N, can be determined by integrating Eq. (1).

$$N = \frac{a_N^{1-\frac{m}{2}} - a_0^{1-\frac{m}{2}}}{C\left(1-\frac{m}{2}\right)\left(\Delta\sigma_h\sqrt{\pi}\right)} \tag{4}$$

The half-crack size can be expressed as a function of N by rewriting Eq. (4).

$$a_N = \left(NC\left(1-\frac{m}{2}\right)\left(\Delta\sigma_h\sqrt{\pi}\right)^m + a_0^{1-\frac{m}{2}}\right)^{\frac{2}{2-m}} \tag{5}$$

The panel will fail when the half-crack size reaches a critical half-crack size, a_c. The critical half-crack size is defined as the size when the stress intensity factor exceeds the plane strain fracture toughness, K_C. The expression for the critical half-crack size is provided in Eq. (6). Note that in the remainder of the paper, crack size refers to the half-crack size.

$$a_C = \left(\frac{K_C}{\sigma_h\sqrt{\pi}}\right)^2 \tag{6}$$

3. Bayesian inference of the damage growth model

Bayesian inference forms a normative and rational method for belief updating when new information is made available. Let the prior distribution about an uncertain event, A, at a state of information, &, be $P(A|\&)$, the likelihood of obtaining an experimental result B given that event A occurred be $P(B|A,\&)$, and the probability of receiving experimental result B (without knowing A has occurred) be $P(B|\&)$. Bayes' rule is used to determine the posterior belief about event A after observing the experiment results, $P(A|B,\&)$, as shown in Eq. (7) [27,28]. Using Bayes' rule, information gained through experimentation can be combined with the prior prediction about the crack size distribution to obtain an updated posterior distribution for the crack size.

$$P(A|B,\&) = \frac{P(A|\&)P(B|A,\&)}{P(B|\&)} \tag{7}$$

Bayesian inference provides a rigorous mathematical framework of belief updating about an unknown variable when new information becomes available. The damage parameters, C and m, in Eq. (1) are normally estimated by fitting fatigue test data measured under controlled, laboratory-environment conditions. Due to potential differences between the test and in-service conditions, there is uncertainty in the tabulated growth parameters. In addition, there is uncertainty in the stress intensity factor range (due to uncertainty in the pressure differential and, therefore, the hoop stress) and the initial crack size, a_0. Bayesian inference assigns a probability distribution to the crack size and takes into account the inherent uncertainty

in the crack growth model. The prior, or initial belief, can be based on theoretical considerations, expert opinions, past experiences, or data reported in the literature; the prior should be chosen to be as informative as possible. The prior is represented as a probability distribution and, using Bayes' theorem, the probability distribution can be updated when new information becomes available (from experiments, for example).

4. Bayesian updating using random walks

Bayesian updating using the random walk approach is explained in this section. From a Bayesian standpoint, an uncertain variable, such as crack size, is treated as a random variable and is characterized by a probability distribution. To generate n sample fatigue crack growth curves (i.e., a_N versus N), samples were selected from the prior joint distribution of m, C, and a_0 (assumed independent) and Eq. (5) was applied. It was considered equally likely that each path represented the true fatigue crack growth curve. Thus, the probability that each sample path was the true crack growth curve was $1/n$. These sample paths were used as the prior in applying Bayesian inference. As noted, the prior can be updated by experimental test results using Bayes' rule. For each sample path, Bayes' rule can be written as:

$$P(\text{path} = \text{true crack growth curve}|\text{test result}, \&) = \frac{P(\text{test result}|\text{path} = \text{true crack growth curve}, \&)}{P(\text{test result}|\&)} P(\text{path} = \text{true crack growth curve}|\&)$$

Here, P(path = true crack growth curve|&) is the prior probability, which before any testing was simply $1/n$ for each sample path, P(test result|path = true crack growth curve|&) is referred to as the likelihood, P(test result|&) is the normalization constant, and P(path = true crack growth curve|test result, &) is the posterior probability that the crack growth curve is the true curve given a test result. From the axioms of probability theory, the area under a probability density function in a continuous case should be equal to unity. Therefore, P(test result|&) acts as a normalization constant of the posterior distribution and need not be calculated separately. According to this equation, the posterior distribution is proportional to the product of the prior and the likelihood. The decision maker should use all available information to generate the prior sample paths, i.e., the crack growth curves. As shown, Bayes' rule is used to update the probability that each sample path is the true crack growth curve using experimental results. For multiple experiments, the posterior after the first update becomes the prior for the second update and so on. Note that the posterior probabilities of each sample path must be normalized so that the sum is equal to unity.

Note that when completing Bayesian updates using the random walk method, the probability that each random sample path is the true path is updated after each measurement. These new sample path probabilities are then used to update the probability distribution of crack size and RUL prediction. This does not require an update of the individual parameter distributions in Paris' law. As an alternative, Monte Carlo simulation can be used to update the parameter distributions and RUL predictions after each measurement. However, this is computationally more expensive. Since the goal is to predict RUL, the intermediate step of updating the uncertain model parameters is eliminated using the random walk method.

In this study, synthetic crack growth data was used to demonstrate the approach. To establish the true crack growth behavior, the values in Table 1 were used, where the applied fuselage pressure differential was taken as 0.06 MPa [29] and m and C were obtained using a crack growth rate plot reported in [30] for 7075-T651 aluminum. The hoop stress range was calculated as $\Delta\sigma_h$ = 78.6 MPa using Eq. (3) and the critical crack size was determined to be a_c = 46.3 mm using Eq. (6). The true crack growth values as a function of the number of cycles were determined using the Table 1 values together with the derived values of $\Delta\sigma_h$ and a_c. As shown in Fig. 1, the critical crack size was reached after 2488 cycles, starting from the initial crack size of 10 mm. The corresponding RUL plot is provided in Fig. 2.

Once the true crack growth behavior was established, the prior joint distribution for the uncertain Paris' law parameters was established and Bayesian updating of this distribution was completed using contrived measurement data to demonstrate the random walk approach.

4.1. Prior

For the prior, n sample paths were generated using random samples from a joint probability density function (pdf) of m, C, and a_0. A large value of n improves the probability that all relevant combinations of these values are included. The sample

Table 1
Parameters for the numerical study.

Parameter	Value	Unit
r	3.25	m
t	0.00248	m
Δp	0.06	MPa
m	3.8	–
C	1.5×10^{-10}	m/cycle
a_0	0.01	m
K_C	30	MPa $\sqrt{m}$

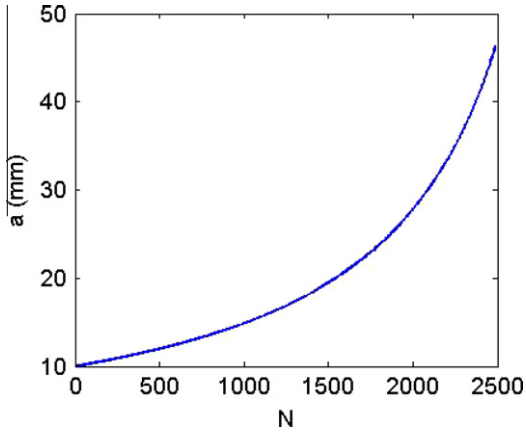

Fig. 1. True crack growth as a function of the number of cycles. The critical crack size is reached in 2488 cycles.

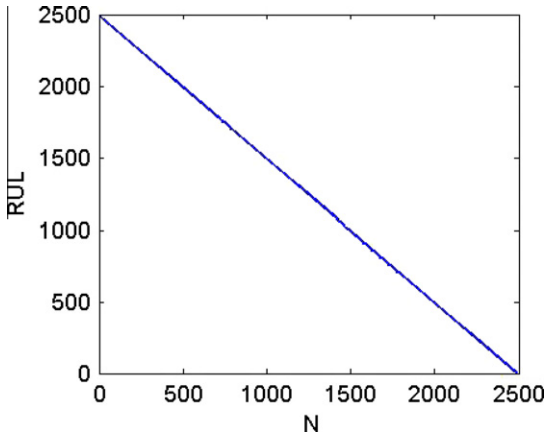

Fig. 2. True RUL at each cycle.

paths representing the prior were generated using Eq. (5). The hoop stress range was assumed to be deterministic (see Table 1). The prior distribution for the damage growth parameters can be determined from laboratory coupon tests or other experimental evidence, finite element analyses, and/or theoretical considerations. In this study, the prior distribution of m, C, and a_0 was assumed to be uniform. The prior joint distribution for the uncertain parameters was selected as [4]: $m = U(3.3,4.3)$, $C = U(5 \times 10^{-11}, 5 \times 10^{-10})$, and $a_0 = U(8,12)$ mm, where U represents a uniform distribution and the parenthetical terms indicate the lower and upper values of the range. The prior m, C, and a_0 distribution was taken as a joint pdf where the parameters were independent of each other. Random samples (1×10^4) were drawn from the prior joint pdf and the fatigue crack growth curve was calculated for each $\{m, C, a_0\}$ sample. Note that uncertainty in a_0 was considered due to measurement bias and noise. The prior distribution of a_0 implies that the initial crack size was equally likely to take any value between 8 mm and 12 mm. According to the prior, each sample fatigue crack growth curve was equally likely to be the true fatigue crack growth curve.

To demonstrate the approach, consider a scenario where $\{m,C\}$ values can take only the 10 different combinations listed in Table 2. Let the initial crack size be 10 mm for illustration purposes. All combinations of $\{m,C\}$ were assumed to be equally likely to be the true combination. This gives a probability of 0.1 for each $\{m,C\}$ pair since there were 10 possible pairs. The fatigue crack growth curves were calculated for the 10 $\{m,C\}$ pairs as a function of N. These are the sample paths, or random walks, each generated using a different $\{m,C\}$ sample. Fig. 3 shows the 10 crack growth curves. The crack size as a function of N was calculated until the crack size reached the critical crack size. Table 2 lists the crack size for each $\{m,C\}$ sample at 1000, 2000, and 3000 cycles. The number of cycles when the crack size reaches the critical crack size, denoted as the number of cycles to failure, N_f, for each sample path is also provided in Table 2. Fig. 4 displays the discrete crack size cumulative distribution function (cdf) at the three intervals. These cdfs give the probability, $p(a)$, of the crack size being less than a selected crack size value as a function of the number of cycles. For example, the probability that the crack size will be less than the critical crack size is 1 at 1000 cycles, 0.7 at 2000 cycles, and 0.4 at 3000 cycles.

There is uncertainty in N_f due to uncertainty in the m and C values. Fig. 5 shows the prior probability that the crack size will be less than the critical crack size as a function of N. These results can be interpreted as follows. From the 10 sample

Table 2
Prior probabilities and tool life for sample $\{m,C\}$ pairs.

Sample	$\{m,C\}$	Crack size (mm)			N_f	Prior
		1000 cycles	2000 cycles	3000 cycles		
1	$\{3.5, 1\times10^{-10}\}$	11.1	12.4	14.1	9021	0.10
2	$\{3.5, 2\times10^{-10}\}$	12.4	16.2	22.4	4510	0.10
3	$\{3.5, 3\times10^{-10}\}$	14.1	22.4	46.1	3007	0.10
4	$\{3.5, 4\times10^{-10}\}$	16.2	34.7	>46.3	2255	0.10
5	$\{3.5, 5\times10^{-10}\}$	18.9	>46.3	>46.3	1804	0.10
6	$\{3.6, 1\times10^{-10}\}$	11.5	13.4	16.1	6720	0.10
7	$\{3.6, 2\times10^{-10}\}$	13.4	19.8	34.8	3360	0.10
8	$\{3.6, 3\times10^{-10}\}$	16.1	34.8	>46.3	2240	0.10
9	$\{3.6, 4\times10^{-10}\}$	19.8	>46.3	>46.3	1680	0.10
10	$\{3.6, 5\times10^{-10}\}$	25.4	>46.3	>46.3	1344	0.10

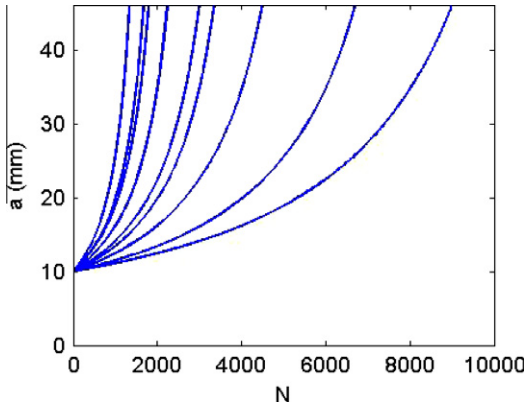

Fig. 3. Sample crack growth curves for the $\{m,C\}$ pairs listed in Table 2.

curves in Fig. 3, zero curves reach the critical crack size before 1343 cycles. Thus, the probability that the crack size is less than the critical crack size is 1 until 1343 cycles. Three curves reach the critical crack size from 1343 cycles to 2000 cycles; these correspond to the $\{3.6, 5\times10^{-10}\}$, $\{3.6, 4\times10^{-10}\}$, and $\{3.5, 5\times10^{-10}\}$ combinations for which the N_f values were 1344, 1680, and 1804 cycles, respectively. Therefore, the probability that the crack size will be less than the critical crack size at 2000 cycles is 0.7 as three equally likely sample curves from the 10 total curves reached the critical crack size. All curves reach the critical crack size before 10,000 cycles. Subsequently, the probability that the crack size will be less than the critical crack size is 0 at 10,000 cycles. The decision maker can estimate the RUL based on an acceptable probability of the crack size reaching the critical crack size.

The procedure was repeated for 1×10^4 sample paths that were generated by drawing random samples from the same prior joint $\{m,C\}$ distribution. The prior probability that any sample curve is the true fatigue crack growth curve was therefore 1×10^{-4}. Recall that uncertainty was assumed in the initial crack size along with the damage growth parameters; the random sample fatigue crack growth curves were equally likely to originate anywhere between 8 mm and 12 mm. As demonstrated, the prior sample paths can be used to determine the cdf of the crack size at any number of cycles in the domain. Fig. 6 shows the crack size cdf at 1000 cycles. From Fig. 6, the probability that the crack size at 1000 cycles will be less than 20.5 mm is 0.5, whereas the probability that the crack size will be less than the critical crack size (46.3 mm) is 0.653. The cdf was then calculated for every cycle in the domain (0 to 10,000). Fig. 7 shows the prior cdf of crack growth as a function of N. Lines of equal probability that the crack size is less than the selected crack size value are provided. Fig. 8 shows the prior probability that the crack size will be less than the critical crack size as a function of N. As expected, the probability of the crack size being less than the critical crack size decreases with N. From Fig. 8, the 95% RUL based on the prior information was 302 cycles. This means that there is a 0.05 probability that the crack size will exceed the critical crack size at 302 cycles.

4.2. Likelihood

According to Bayes' rule, the posterior distribution is proportional to the product of the prior and likelihood functions. This section explains the likelihood function formulation. There is crack size uncertainty due to uncertainties in the underlying model and the presence of bias and noise in crack size measurements. The user can estimate the uncertainties in the crack size measurements based on his/her beliefs about the SHM system. To illustrate, consider a crack size measurement of 16.2 mm after 1000 cycles. Based on the measurement result and the measurement and model uncertainties, the user might believe that it is very likely that the true crack size is between 15.2 mm and 17.2 mm. The user may also estimate that it is

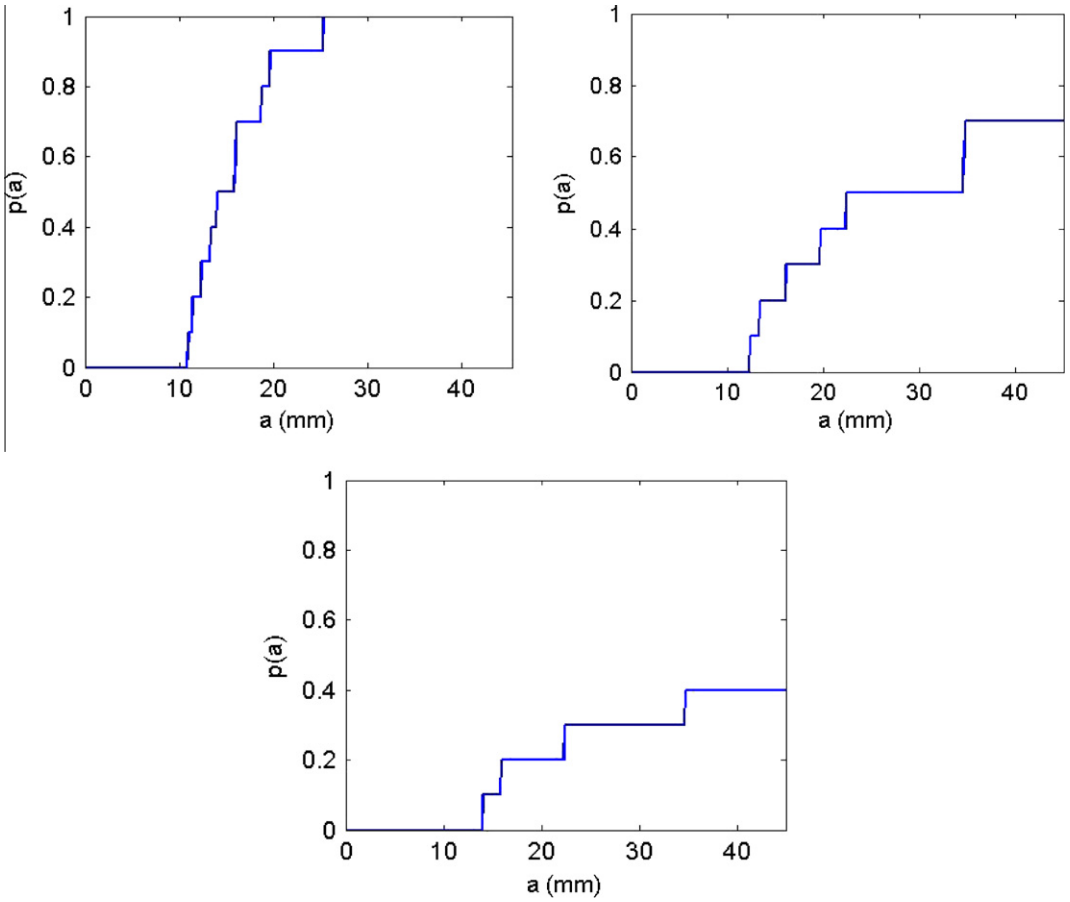

Fig. 4. Prior cdf of crack size at 1000 cycles (top left), 2000 cycles (top right), and 3000 cycles (bottom left).

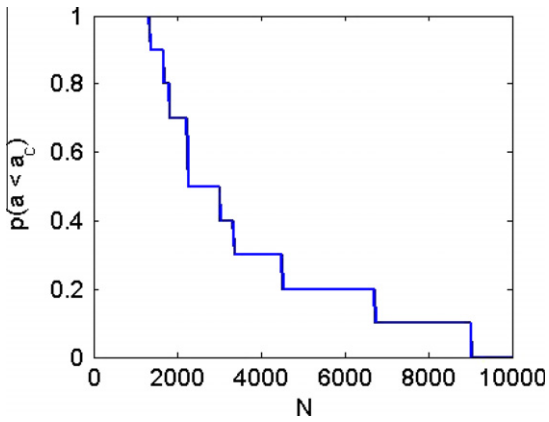

Fig. 5. Prior probability of the crack size being less than the critical crack size as a function of the number of cycles.

unlikely that the true crack size was less than 13.2 mm or greater than 19.2 mm, for example. The likelihood function takes into account these beliefs. See Eq. (8), where l is the likelihood function, a_{meas} is the measured crack size, a is the crack size for a sample fatigue crack growth curve at measurement N, and k is a parameter that describes the function spread. (Recall that crack size actually denotes the half-crack size.)

$$l = e^{\frac{-(a-a_{meas})^2}{k}} \tag{8}$$

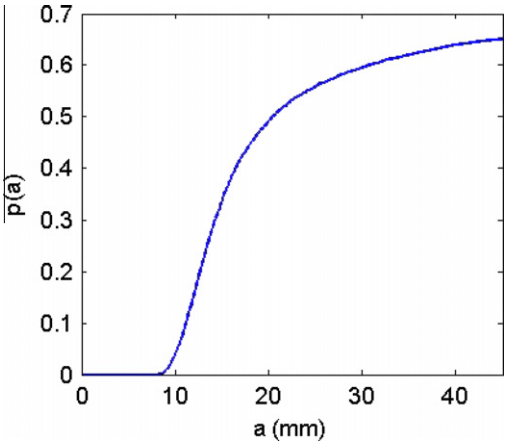

Fig. 6. Prior cdf of crack size at 1000 cycles.

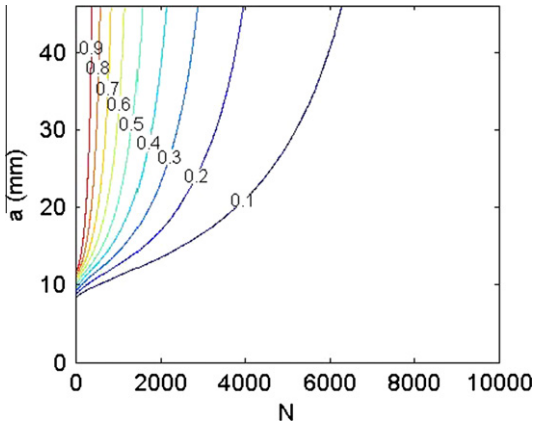

Fig. 7. Prior cdf of crack size.

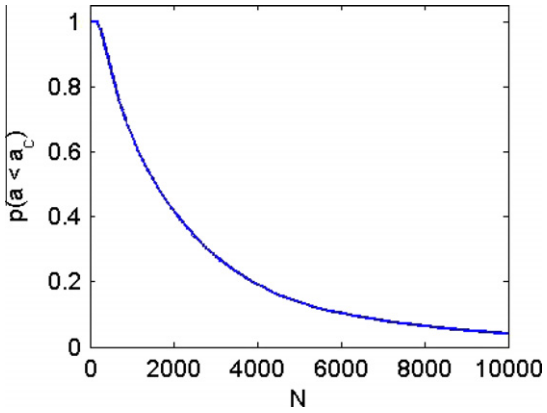

Fig. 8. Prior probability that the crack size is less than the critical crack size as a function of *N*.

The likelihood function is expressed as a non-normalized normal distribution, where the parameter $k = 2\sigma^2$ and σ is the standard deviation of crack size (due to measurement, material, and model uncertainty). The value of k is estimated by the user based on his/her beliefs. The likelihood function describes how likely it is that each sample path is the true crack growth curve based on the measured value. If the fatigue crack growth curve value is near the measurement result, then the likelihood value is high. Otherwise, it is low. The likelihood function defined in Eq. (8) does not reject sample paths which differ

significantly from the measurement result; it simply assigns them a small weighting factor. To demonstrate, again consider the 10 possible $\{m,C\}$ pairs listed in Table 2. Assume that a crack size measurement of 16.2 mm was obtained at 1000 cycles. Each sample fatigue crack growth curve has a crack size value that depends on the $\{m,C\}$ pair used to generate the sample path (see Table 2). The likelihood function can be interpreted as assigning weights from zero to unity for these sample paths, where zero indicates that the combination is not likely at all and unity identifies the most likely combination. The likelihood for each sample fatigue crack growth curve was calculated using Eq. (8). The likelihood can also be modified to incorporate the presence of a bias in the measured crack size in addition to uncertainty; see Eq. (9), where b_1 and b_2 define the bias in the measured crack size as estimated by the user.

$$l = \begin{cases} e^{\frac{-(a-(a_{meas}-b_1))^2}{k}} & a < a_{meas} - b_1 \\ 1 & a_{meas} - b_1 \leqslant a \leqslant a_{meas} + b_2 \\ e^{\frac{-(a-(a_{meas}+b_2))^2}{k}} & a > a_{meas} + b_2 \end{cases} \tag{9}$$

The value of σ (or k) in the likelihood function is estimated by the user based on his/her beliefs about the model uncertainty and the presence of noise and bias in the sensor measurement. If the user believes a positive or negative bias may exist, the values of b_1 and b_2 in Eq. (9) are selected accordingly. For example, if the user estimates a negative bias in the sensor measurement, the value of b_2 would be assigned by the user and b_1 would be 0. For a positive bias, the value of b_1 would be assigned by the user and b_2 would be 0. Table 3 lists the likelihood values for the 10 possible $\{m,C\}$ pairs with a measured

Table 3
Likelihood probabilities for sample $\{m,C\}$ pairs given a measured crack size of 16.2 mm at 1000 cycles.

Sample	$\{m,C\}$	Crack size (mm)			N_f	Prior	Likelihood
		1000 cycles	2000 cycles	3000 cycles			
1	$\{3.5, 1\times10^{-10}\}$	11.1	12.4	14.1	9021	0.10	2.46×10^{-6}
2	$\{3.5, 2\times10^{-10}\}$	12.4	16.2	22.4	4510	0.10	9.19×10^{-4}
3	$\{3.5, 3\times10^{-10}\}$	14.1	22.4	46.1	3007	0.10	0.113
4	$\{3.5, 4\times10^{-10}\}$	16.2	34.7	>46.3	2255	0.10	1.000
5	$\{3.5, 5\times10^{-10}\}$	18.9	>46.3	>46.3	1804	0.10	0.027
6	$\{3.6, 1\times10^{-10}\}$	11.5	13.4	16.1	6720	0.10	1.60×10^{-5}
7	$\{3.6, 2\times10^{-10}\}$	13.4	19.8	34.8	3360	0.10	0.022
8	$\{3.6, 3\times10^{-10}\}$	16.1	34.8	>46.3	2240	0.10	0.992
9	$\{3.6, 4\times10^{-10}\}$	19.8	>46.3	>46.3	1680	0.10	0.001
10	$\{3.6, 5\times10^{-10}\}$	25.4	>46.3	>46.3	1344	0.10	3.18×10^{-19}

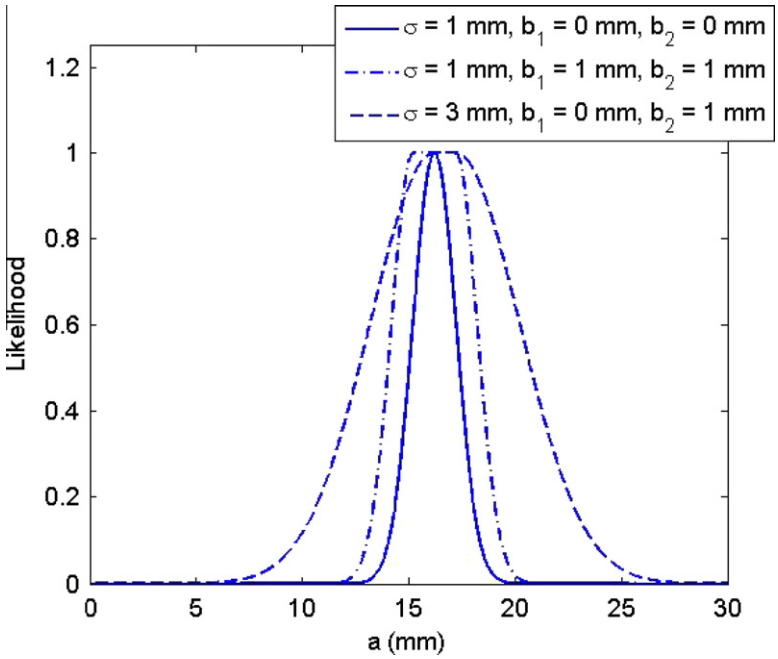

Fig. 9. Example likelihood functions for a crack size measurement of 16.2 mm after 1000 cycles.

crack size of 16.2 mm at 1000 cycles. For the likelihood calculation, the value of σ, b_1, and b_2 were taken as 1 mm, 0 mm, and 0 mm, respectively. The likelihood values listed in Table 3 show that $\{3.5, 4 \times 10^{-10}\}$ was most likely to be the correct $\{m,C\}$ combination, while $\{3.6, 5 \times 10^{-10}\}$ was the least likely. Fig. 9 shows the likelihood function for $a_{meas} = 16.2$ mm at 1000 cycles for different σ, b_1, and b_2 values. As seen in the figure, increased uncertainty (higher σ and/or b_1 or b_2) broadens the likelihood function so that comparatively higher weights are assigned to sample curves further from the experimental result. Subsequently, larger uncertainty yields a conservative estimate of crack size and, therefore, RUL. The effect of estimated values of σ, b_1, and b_2 on the RUL is discussed in Section 5. Although the values for σ, b_1, and b_2 are considered constant in this study, they could also be expressed as a function of N.

5. Bayesian updating

The posterior distribution is obtained by a (normalized) multiplication of the prior and likelihood functions. The prior probability of each sample path in this study was 1×10^{-4}. The likelihood probability was calculated using Eq. (8). The posterior probability for 10 sample paths is provided in Table 4. Recall that in the illustration example, the initial crack size was assumed to be 10 mm. For this first update, the measured crack size was 16.2 mm at 1000 cycles. For the likelihood calculation, the value of σ, b_1, and b_2 were taken as 1 mm, 0 mm, and 0 mm, respectively. For each N, the updated probabilities of sample fatigue curves provide an updated crack size distribution. Therefore, a crack size measurement at a selected cycle updates the crack size distribution at all cycles. Fig. 10 displays updated posterior crack size distributions at 1000, 2000, and 3000 cycles given the crack size measurement of 16.2 mm at 1000 cycles (solid lines). Fig. 10 also includes the prior crack size cdfs for comparison (dashed lines). Fig. 11 shows the posterior probability that the crack size will be less than the critical crack size as a function of N. Note that for the posterior cdf calculation, the updated probabilities, or weights, of the sample paths must be considered. From Fig. 11, it is seen that there was an improvement in the posterior probability of the crack size reaching the critical crack size.

The Bayesian updating procedure was repeated for all 1×10^4 sample paths. Fig. 12 shows a comparison between prior and posterior cdf of crack size at 1000 cycles. From the posterior cdf, the probability that the crack size is less than the critical crack size (46.3 mm) is 1 at 1000 cycles. Fig. 13 shows the updated posterior distribution given $a_{meas} = 16.2$ mm at 1000 cycles. Fig. 14 shows a comparison between the prior and posterior probability that the crack size will be less than critical crack size as a function of N. It is observed that there is a 0.05 probability that the crack size will exceed the critical crack size at 1704 cycles. Since the measurement is at 1000 cycles, the RUL at 1000 cycles was 704 cycles. Therefore, the RUL estimate was updated using a measurement result.

In certain cases, the posterior distribution for the uncertain parameters may be required because these distributions can be used to generate the prior for another group of fuselage panels. Recall that each sample fatigue crack growth curve was generated using a sample of $\{m, C, a_0\}$. For the prior, each sample fatigue crack growth curve was assumed to equally likely to be the true curve; this implies that each $\{m, C, a_0\}$ combination used to generate the sample curve was equally likely to be the true combination. The updated probability of each sample curve gives the updated probability of the underlying $\{m, C, a_0\}$ sample to be the true combination. The mean, standard deviation, and correlation coefficient of the parameters can be determined from the posterior probabilities using the following relations:

$$\mu_m = \sum mP(m) = 3.801 \tag{10a}$$

$$\mu_C = \sum CP(C) = 2.68 \times 10^{-10} \tag{10b}$$

$$\sigma_m = \sum (m - \mu_m)^2 P(m) = 0.286 \tag{10c}$$

$$\sigma_C = \sum (C - \mu_C)^2 P(C) = 1.28 \times 10^{-10} \tag{10d}$$

Table 4
Posterior probabilities for sample $\{m,C\}$ pairs after the first update.

Sample	$\{m,C\}$	Prior	Likelihood	Posterior (non-normalized)	Posterior (normalized)
1	$\{3.5, 1 \times 10^{-10}\}$	0.10	2.46×10^{-6}	2.46×10^{-7}	1.14×10^{-6}
2	$\{3.5, 2 \times 10^{-10}\}$	0.10	9.19×10^{-4}	9.19×10^{-5}	4.26×10^{-6}
3	$\{3.5, 3 \times 10^{-10}\}$	0.10	0.113	0.0113	0.052
4	$\{3.5, 4 \times 10^{-10}\}$	0.10	1.000	0.1	0.464
5	$\{3.5, 5 \times 10^{-10}\}$	0.10	0.027	0.0027	0.012
6	$\{3.6, 1 \times 10^{-10}\}$	0.10	1.60×10^{-5}	1.60×10^{-6}	7.42×10^{-6}
7	$\{3.6, 2 \times 10^{-10}\}$	0.10	0.022	0.0022	0.010
8	$\{3.6, 3 \times 10^{-10}\}$	0.10	0.992	0.0992	0.460
9	$\{3.6, 4 \times 10^{-10}\}$	0.10	0.001	0.0001	4.64×10^{-4}
10	$\{3.6, 5 \times 10^{-10}\}$	0.10	3.18×10^{-19}	3.18×10^{-20}	1.48×10^{-19}
				$\Sigma = 0.215$	$\Sigma = 1.00$

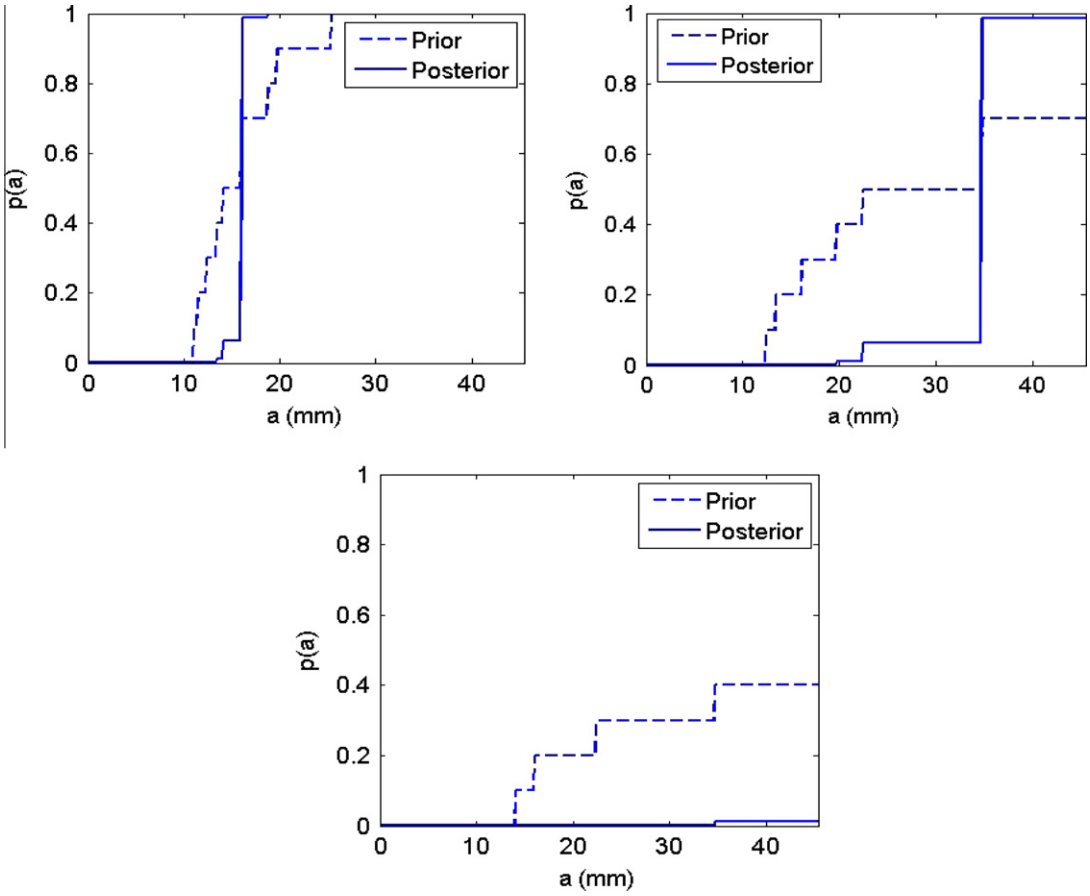

Fig. 10. Posterior cdf of crack size at 1000 (top left), 2000 (top right), and 3000 cycles (bottom left) using a measured crack size of 16.2 mm at 1000 cycles.

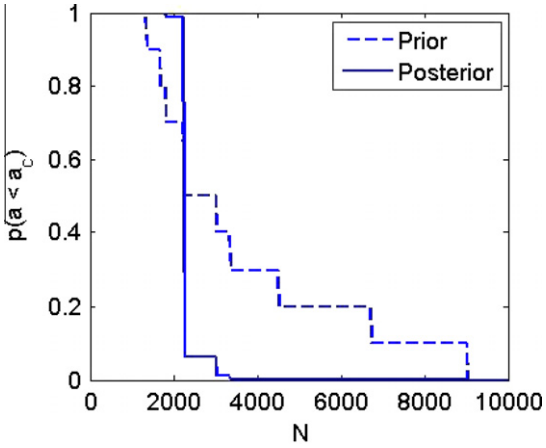

Fig. 11. Posterior probability that the crack size is less than the critical crack size as a function of *N*.

$$\rho_{m,C} = \frac{\sum mCP(m,C) - \mu_m \mu_C}{\sigma_m \sigma_C} = 0.0541 \tag{10e}$$

In these equations, the summations were carried out over all n samples, where $P(m)$, $P(C)$, and $P(m,C)$ are the posterior probabilities for m, C, and the $\{m,C\}$ pairs, respectively; μ_m and μ_C are the mean values of m and C, respectively; σ_m and σ_C are the standard deviations of m and C, respectively; and $\rho_{m,C}$ is the correlation coefficient between m and C. The terms $P(m)$, $P(C)$, and $P(m,C)$ are equal to the posterior probabilities of the sample curves. For the numerical study provided here,

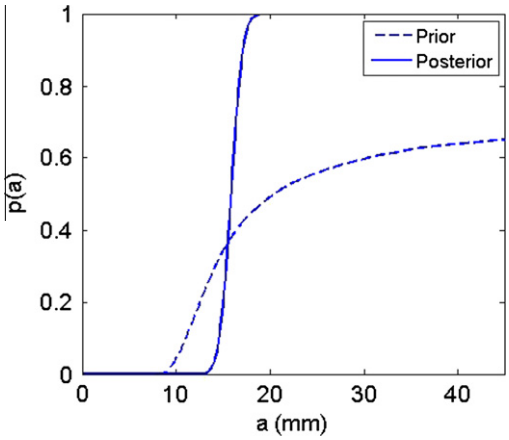

Fig. 12. Prior and posterior cdfs of crack size at 1000 cycles.

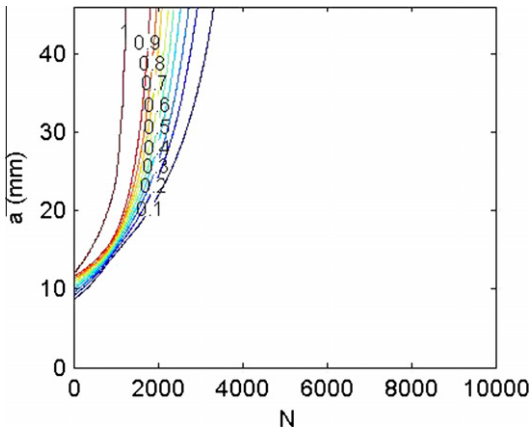

Fig. 13. Posterior cdf of crack size as a function of *N*.

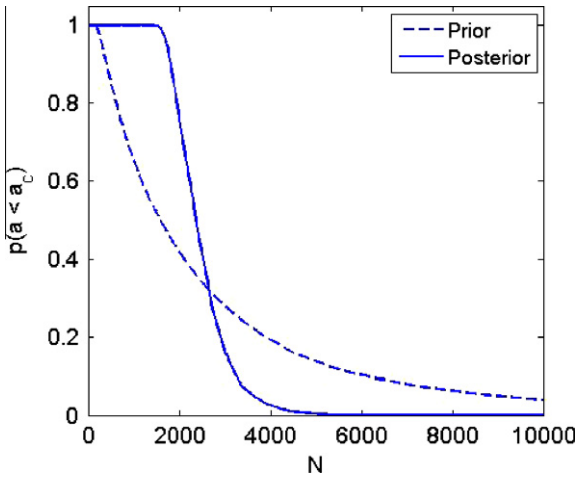

Fig. 14. Posterior and prior probability that the crack size is less than the critical crack size as a function of *N*.

the mean value of m was close to the true value, while the mean value of C was not. This is because the value of C is very sensitive to the value of the exponent m. As a result, the standard deviation of C was high. The true value of C was within one standard deviation of the mean value. Eqs. (10a)–(10e) can also be modified to determine the mean and standard deviation of a_0 and its correlation coefficients with m and C, respectively.

6. Prediction of RUL

The posterior probabilities of the sample paths after each update were used to predict the RUL. The crack size measurement values were calculated using the true parameter values listed in Table 1. It was assumed that the crack size measurements were performed at 100 cycle intervals, which resulted in 24 total measurements and subsequent updating of the crack size distribution. A 95% RUL was used in this study, where there is a 0.05 probability of the crack size reaching the critical crack size at the 95% RUL value. The 95% RUL was then compared with the true RUL (see Fig. 2). To simulate real measurement conditions and incorporate the model uncertainty, a bias, B, and standard normal random noise were added to the true crack size. The uncertainty was described using $N(M, S^2)$, where N denotes a normal distribution, M is the mean, and S is the standard deviation. In the first analysis, no bias or noise was added to the simulated crack size measurement values ($B = 0, S = 0$). The crack size value was calculated at 100 cycle intervals and used to update the crack size distribution. The value of σ, as estimated by the user in the likelihood function (Eq. (8)), was 1 mm. The 95% RUL after 2400 cycles was calculated as 67 cycles using the procedure described in Section 4; the true RUL was 88 cycles. The result was conservative because uncertainty in the measured crack size values was considered in the likelihood function. The mean and standard deviation for the posterior $\{m, C, a_0\}$ distributions were $\{3.82, 0.28\}$ for m, $\{2.52 \times 10^{-10}, 1.46 \times 10^{-10}\}$ for C, and $\{10.0, 9.5 \times 10^{-4}\}$ mm for a_0. The correlation coefficients were -0.567 between m and C, 0.62 between m and a_0, and -0.46 between a_0 and C. The Paris' law parameters show a strong correlation, as expected [31,32].

Next, noise with $S = 1$ mm was added to the true crack size. The value of σ was again 1 mm. Fig. 15 shows the true crack growth curve and the simulated values for a single set of measurements. After each update, the 95% RUL value was calculated. The RUL prediction may vary with different samples of the simulated crack size values since random noise was added to the simulated crack size values. The process was repeated for 100 sets of 24 measurements. Fig. 16 shows the 95% RUL prediction for all 100 sets of measurements. It is seen that there was a gradual improvement in the RUL prediction with each measurement. The prior uncertainty in the values of m, C, and a_0, ($m = U(3.3, 4.3)$, $C = U(5 \times 10^{-11}, 5 \times 10^{-10})$ and $a_0 = U(8, 12)$ mm), was large which resulted in a conservative prediction at the start. Fig. 17 shows the histogram of the predicted RUL from the 100 sets of measurements at 2400 cycles, which was the last update, and the true RUL. Since the assumed likelihood uncertainty was equal to the true uncertainty ($S = \sigma = 1$ mm), a 95% RUL prediction resulted in a 5% non-conservative prediction of RUL. Fig. 17 shows that the RUL prediction was non-conservative for six of the 100 measurement sets. Fig. 18 shows the 99% RUL for all 100 sets of measurement (left) and the histogram of 99% RUL (right). A 99% RUL prescribes that there is a 0.01 probability that the crack size will reach the critical crack size. As expected, the 99% RUL leads to a conservative estimate as compared to the 95% RUL.

In practice, the true value of S is unknown to the user. It is estimated in the likelihood calculation (σ) based on his/her beliefs. The values estimated by the user can therefore be different than the true value, which affects the RUL predictions. This was evaluated by considering the three cases in Table 5. For Case 1, the estimated uncertainty was equal to the true uncertainty ($S = \sigma = 1$ mm). For Case 2, the uncertainty estimated by the user ($\sigma = 3$ mm) was higher than the true value of noise ($S = 1$ mm). For Case 3, the uncertainty estimated by the user ($\sigma = 1$ mm) was lower than the true value ($S = 3$ mm). The Case 2 and 3 results were compared to Case 1 (see Fig. 16). Fig. 19 shows the 95% RUL prediction for Case 2 (left) and Case 3 (right). Fig. 20 shows the histogram of RUL at 2400 cycles for Case 2 (left) and Case 3 (right). As expected, a higher estimate of the uncertainty (Case 2) results in a more conservative RUL prediction, while a lower estimate (Case 3) results in a non-conservative prediction of RUL.

Next, the effect of bias in the crack size measurements on the RUL prediction was evaluated. Two cases were considered. First, a bias of 1 mm ($B = 1$ mm) was added to the true crack size along with a noise standard deviation equal to 1 mm ($S = 1$ mm). The likelihood standard deviation was also taken as 1 mm and the bias was zero ($b_1 = b_2 = 0$ in Eq. (9)). Second,

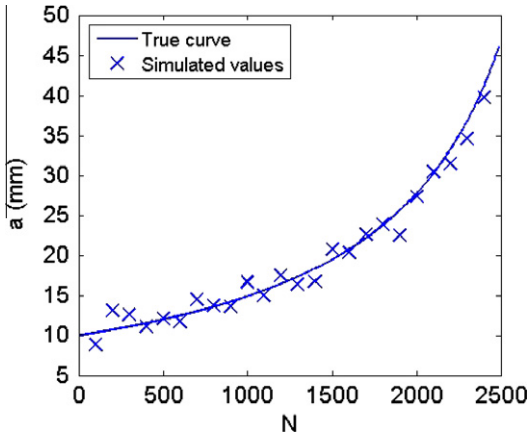

Fig. 15. True crack growth curve and the simulated values used for updating using a single set of measurements.

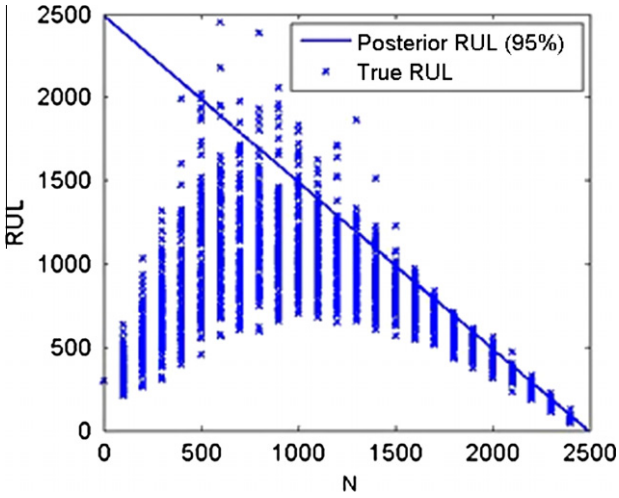

Fig. 16. 95% RUL prediction for all 100 sets of measurements.

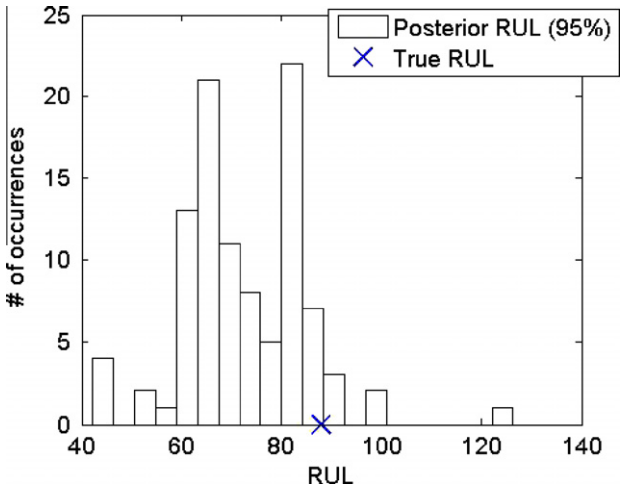

Fig. 17. Histogram of the predicted 95% RUL at 2400 cycles.

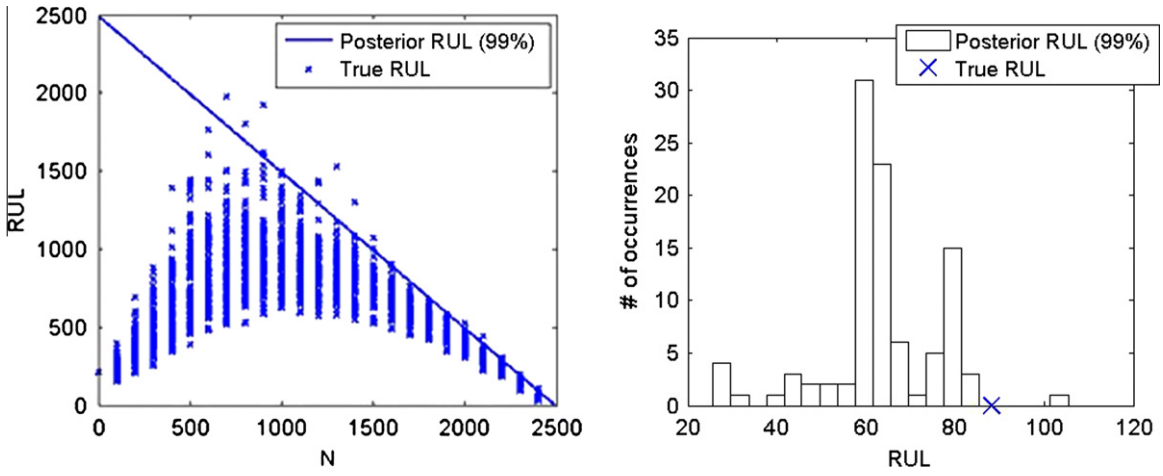

Fig. 18. 99% RUL prediction for all 100 sets of measurements (left) and histogram of the predicted 99% RUL at 2400 cycles (right).

Table 5
Three cases to evaluate the effect of uncertainty estimate.

Case	S (mm)	σ (mm)
1	1	1
2	1	3
3	3	1

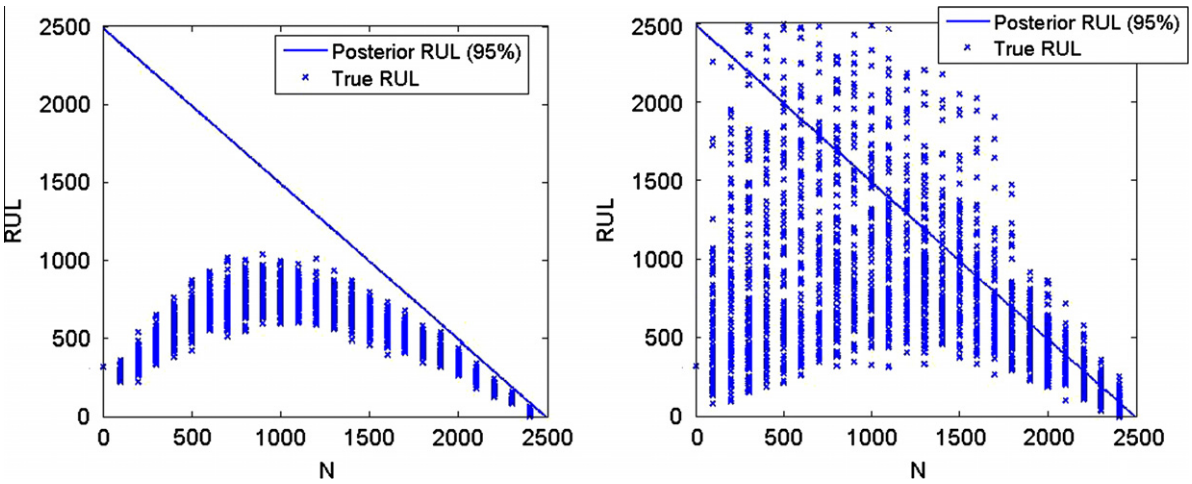

Fig. 19. 95% RUL prediction for all 100 sets of measurements for Case 2 (left) and Case 3 (right).

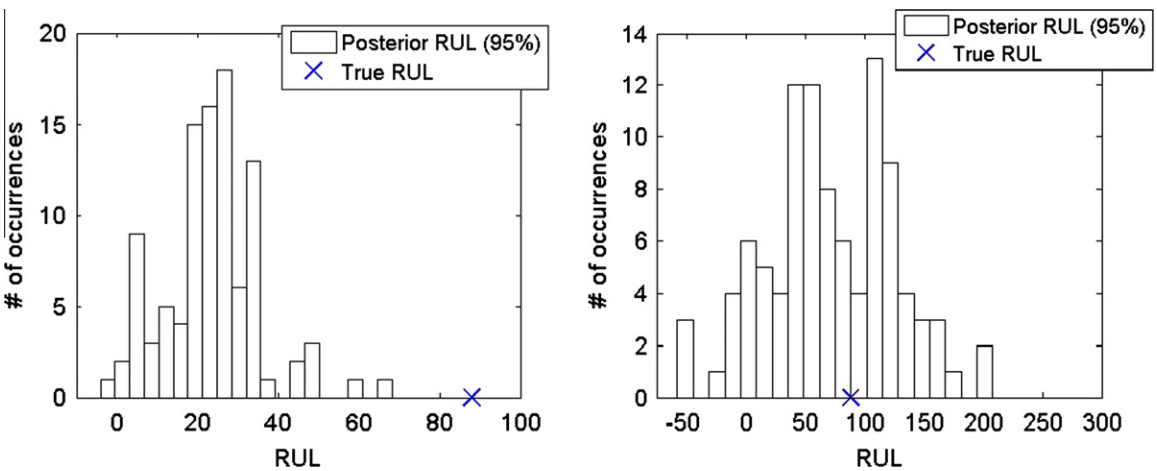

Fig. 20. Histogram of the predicted 95% RUL at 2400 cycles for Case 2 (left) and Case 3 (right).

a bias of -1 mm ($B = -1$ mm) was added to the true crack size. Fig. 21 shows the histogram of RUL at 2400 cycles for $B = 1$ mm (left) and $B = -1$ mm (right). A positive bias along with noise in the measurement leads to a conservative prediction of RUL, while a negative bias leads to a non-conservative prediction.

As noted, a bias can be incorporated in the likelihood function using two parameters, b_1 and b_2. A negative bias should be accounted for as it leads to a non-conservative prediction of RUL. Two cases were considered to incorporate bias in the likelihood. In the first case, the uncertainty in the likelihood was 1 mm ($\sigma = 1$ mm) and the bias was 1 mm ($b_1 = 1$ mm and $b_2 = 1$ mm). The values of S and B were 1 mm and -1 mm, respectively. A comparison of the right panel of Fig. 21 (no bias in the likelihood) and the left panel of Fig. 22 (bias included) shows that incorporating the bias yields a more conservative result. In the second case, an uncertainty of 3 mm was assumed in the likelihood ($\sigma = 3$ mm) and bias was not considered ($b_1 = 0$ and $b_2 = 0$). The values of S and B were again 1 mm and -1 mm, respectively. By comparing the right panel of Fig. 21 ($\sigma = 1$ mm) and the right panel of Fig. 22 ($\sigma = 3$ mm), it is seen that the RUL prediction was conservative for the

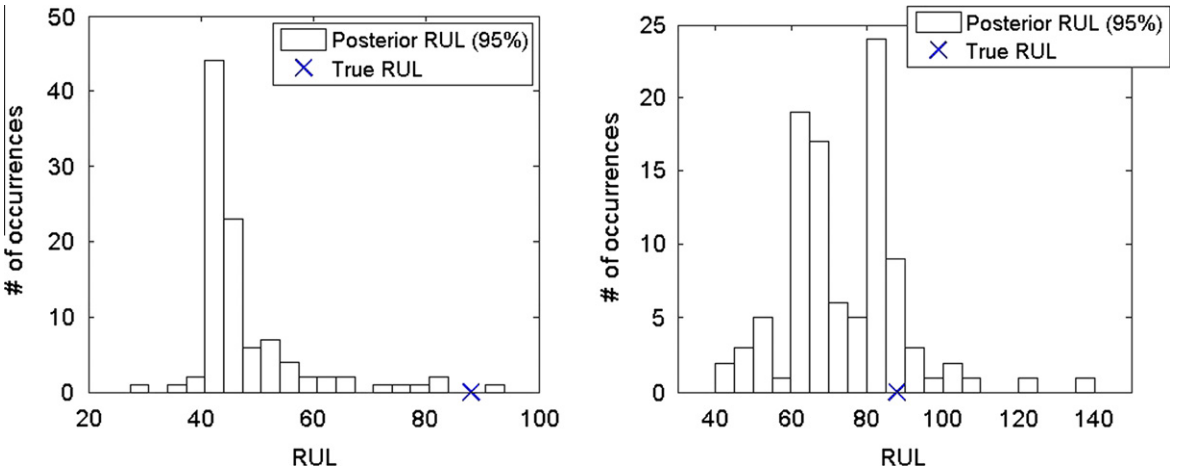

Fig. 21. Histogram of the predicted 95% RUL at 2400 cycles for $B = 1$ mm (left) and $B = -1$ mm (right). The value of both S and σ was 1 mm.

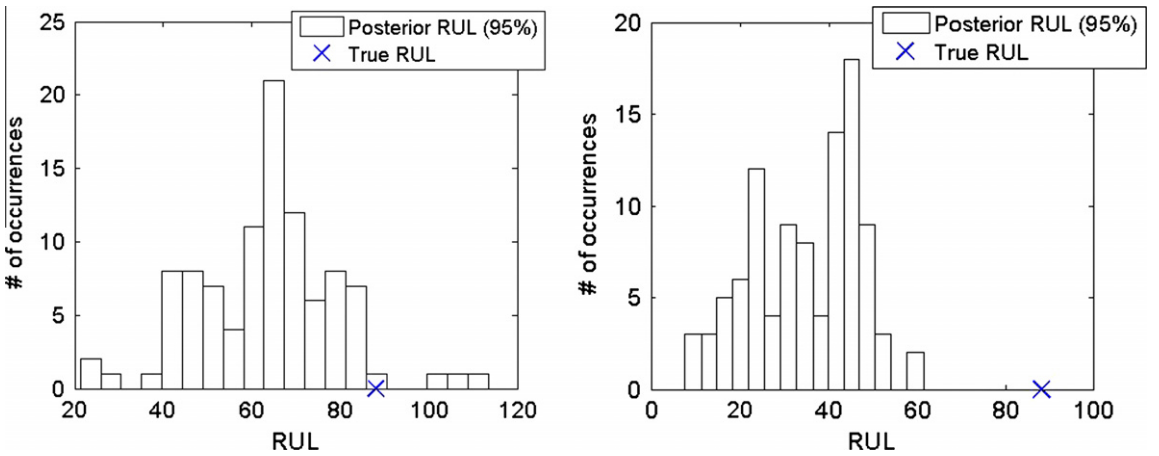

Fig. 22. Histogram of the predicted 95% RUL at 2400 cycles for $\sigma = 1$ mm, $b_1 = 1$ mm and $b_2 = 1$ mm (left) and $\sigma = 3$ mm, $b_1 = 0$ mm and $b_2 = 0$ mm (right). The values of S and B were 1 mm and -1 mm, respectively.

$\sigma = 3$ mm case. This follows from the results of Fig. 9 (based on Eq. (9)) that depicts a broader likelihood function with increasing σ. Therefore, a higher likelihood value is assigned to all sample paths.

7. Advantages

Bayesian inference using the random walk method offers many advantages. In the random walk methodology the individual damage growth parameter distributions are not updated. Instead, the probability that each sample path is the true fatigue crack growth curve is updated. In contrast, the joint distributions of parameters and RUL may be updated by Monte Carlo simulation after each measurement, but this can be computationally expensive. Since the goal is predicting RUL, the intermediate step of calculating posterior parameter distributions after each update is unnecessary and is eliminated in the technique described here. In cases where the posterior distributions of the uncertain parameters are required, they can be determined as shown in Eqs. (10a), (10b), (10c), (10d), (10e). In the random walk method, the prior sample paths, or sample curves, need to be generated only once and the probability of each curve being the true curve is updated. Therefore, the method enables uncertainty in input variables, such as the initial crack size, pressure differential, and growth parameters, to be considered in the prior. Without loss of generality, the same procedure is also applicable for advanced fatigue crack growth models with additional parameters. The advantages of the method exist for higher reliability RUL problems. The computation time depends on the time required to generate the sample curves; therefore it might be a factor for time consuming crack growth analysis using retardation modeling. Note that the prior sample curves need to be generated only once. Using the approach described here, the effectiveness of different models can be evaluated using reported fatigue crack growth data [33,34].

The presence of a bias in the measurement may cause a shift in the posterior distributions of parameters, which can lead to over/under estimation of RUL. The likelihood function presented in this work can incorporate the presence of noise and bias, along with the model uncertainties, and it is straightforward to calculate. The likelihood need not be a standard distribution; it can be defined by the user based on his/her beliefs. Additionally, there is no need to use conjugate distributions. For Bayesian updating in general, it is preferred to use conjugate distributions for the prior and likelihood, such as normal-normal and Bernoulli-beta, for convenience in calculations and sampling from the posterior distributions. If conjugate distributions are not used for the prior and the likelihood, the posterior is not a standard distribution. Sampling from a non-standard distribution makes the updating procedure computationally expensive or, in some cases, infeasible. Sampling errors from the posterior distribution would also affect the RUL predictions. However, in the case of updating using the random walk method, the likelihood can be chosen to be any distribution, such as triangular, stepped, or one-sided. It does not need to be a conjugate distribution with the prior. The choice of the likelihood function does not affect the updating procedure. The only consideration is that, since the likelihood is based on the user's beliefs, the effect of the likelihood spread on RUL should be evaluated.

8. Conclusions

The application of Bayesian inference to remaining useful life prediction in fatigue-damaged structures was demonstrated using a random walk approach. In Bayesian inference, a probability distribution is assigned over a range of the variable(s) of interest and the distribution is updated when new information becomes available. Using this new information, uncertainty in the prior distribution can be reduced. Bayesian inference therefore provides a way to combine prior data with experimental results to update beliefs about an uncertain variable. Using the random walk approach, the prior probability of crack size was generated using sample fatigue crack growth curves, where each path represented the true fatigue crack growth curve with some probability. This probability was updated using Bayesian inference. A likelihood function was defined to describe how likely it was that that the sample fatigue crack growth curve represented the correct curve given the measurement result at a particular cycle number. Bayesian inference can be combined with decision analysis models to assign a dollar value to information gained from an experiment prior to performing it. This value is referred to as the *value of information*. For follow-on research, the value of information approach can be used to determine the optimum number of cycles before the structure is scheduled for maintenance based on the user's preferences.

References

[1] Farrar CR, Worden K. An introduction to structural health monitoring. Philos Trans Royal Soc 1851;2007(365):303–15.
[2] Sohn H, Farrar CR, Hemez, FM, Czarnecki JJ. A review of structural health monitoring literature, 1996–2001. In: Third world conf. on struct control, Como, Italy, April 7–12 2002.
[3] Loh KJ, Lynch JP. Summary review of wireless sensors and sensor networks for SHM. Shock Vib Dig 2006;38(2):91–128.
[4] Coppe A, Haftka RT, Kim NH, Yuan F. Uncertainty reduction of damage growth properties using structural health monitoring. J Aircraft 2010;47(6):2030–8.
[5] Engel SJ, Gilmartin BJ, Bongort K, Hess A. Prognostics: the real issues involved with predicting life remaining. In: IEEE aerosp conf., vol. 6. 2000. p. 456–67.
[6] Newman Jr JC. Prediction of fatigue crack growth under variable-amplitude and spectrum loading using a closure model, vol. 761. Am Soc Test Mater STP; 1982. p. 255–77.
[7] Newman Jr JC. A crack-opening stress equation for fatigue crack growth. Int J Fract 1984;24:R131–5.
[8] Ray A, Patankar RP. Fatigue crack growth under variable amplitude loading. Part I: Model formulation in state-space setting. Appl Math Model J 2001;25(11):979–94.
[9] Ray A, Patankar RP. Fatigue crack growth under variable amplitude loading. Part II: Code development and model validation. Appl Math Model J 2001;25(11):995–1013.
[10] Wu WF, Ni CC. A study of stochastic crack growth modeling using experimental data. Probab Engng Mech 2003;18:107–18.
[11] Wu WF, Ni CC. Statistical aspects of some fatigue crack growth data. Engng Fract Mech 2007;74:2952–63.
[12] Ortiz K, Kiremidjian AS. Stochastic modeling of fatigue crack growth. Engng Fract Mech 1988;29(3):317–34.
[13] Langley RS. Stochastic models of fatigue crack growth. Fract Mech 1989;32(1):137–45.
[14] Ditlevsen O, Olsen R. Statistical analysis of the Virkler data on fatigue crack growth. Fract Mech 1986;25(2):176–95.
[15] Ray A, Tangirala S. Stochastic modeling on fatigue crack dynamics for on-line failure prognostics. IEEE Trans Control Syst Technol 1996;4(4):443–51.
[16] Orchard M, Kacprzynski G, Goebel K, Saha B, Vachtsevanos, G. Advances in uncertainty representation and management for particle filtering applied to prognostics. In: Int conf on progn and health manag, vol. 1, October 6–9, 2008. Denver, Co p. 6.
[17] Liang T, DeCastro J, Kacprzynski G, Goebel K, Vachtsevanos G. Filtering and prediction techniques for model-based prognosis and uncertainty management. In: Int conf on progn and health manag, January 12–14, 2010. Macao, p. 1–10.
[18] Cadini F, Zio E, Avram D. Monte Carlo-based filtering for fatigue crack growth estimation. Probab Engng Mech 2009;24:367–73.
[19] Perrin F, Sudret B, Pendola M. Bayesian updating of mechanical models - application in fracture mechanics. In: 18 ème Congrès Français de Mécanique, Grenoble, August 27–31 2007.
[20] Mohanty S, Chattopadhyay A, Peralta P, Das S. Bayesian statistic based multivariate gaussian process approach for offline/online fatigue crack growth prediction. Exp Mech 2010;51:833–43.
[21] Zhang R, Mahadevan S. Model uncertainty and Bayesian updating in reliability-based inspection. J Struct Saf 2000;22:145–60.
[22] Paris PC, Erdogan F. A critical analysis of crack propagation laws. J Basic Engng ASME 1960;34:528–34.
[23] Paris PC, Tada H, Donald JK. Service load fatigue damage – a historical perspective. Int J Fatigue 1999;21:35–46.
[24] Zhao Z, Haldar A. Reliability-based structural fatigue damage evaluation and maintenance using non-destructive inspections. Uncertain Model in fatigue elem, fatigue and stab of syst. New York: World Scientific; 1997. p. 159-214.
[25] Byers WG, Marley MJ, Mohammadi J, Nielsen RJ, Sarkani S. Fatigue reliability reassessment procedures: state-of-the art paper. J Struct Engng ASCE 1997;123(3):271–6.
[26] Lin KY, Rusk DT, Du JJ. Equivalent level of safety approach to damage-tolerant aircraft structural design. J Aircraft 2002;39:167–74.
[27] Gelman A, Carlin JB, Stern HS, Rubin DB. Bayesian data analysis. 2nd ed. Boca Raton (FL): Chapman and Hall/CRC Press; 2009.

[28] Grimmett GR, Stirizaker DR. Probability and random processes. New York, NY: Oxford Univ Press; 2009.
[29] Newman J. Crack growth under variable amplitude and spectrum loading. In: TMS symp proc. to honor P. Paris, Indianapolis, September 14–18, 1997.
[30] Niu M. Airframe structural design. Hong Kong: Conmilit Press; 1990. 538–570.
[31] Annis C. Probabilistic life prediction isn't as easy as it looks. In: Johnson WS, Hillberry BM, editors. Spec tech proc. West Conshohocken (PA): ASTM Int; 2003. p. 1450.
[32] Carpinteri A, Paggi M. Are the Paris' law parameters dependent on each other? Fratt Integr Strut 2007;2:10–6.
[33] Virkler DA, Hillberry BM, Goel PK. The statistical nature of fatigue crack propagation. J Engng Mater Techno ASME 1979;101:148–52.
[34] Ghonem H, Dore S. Experimental study of the constant-probability crack growth curves under constant amplitude loading. J Eng Fract Mech 1987;27(1):1–25.